

# Energy Dispersive, X-ray Fluorescence Analysis

**Peter Wobrauschek and Christina Strelj**

*Atominstytut, Vienna University of Technology, Vienna, Austria*

**Eva Selin Lindgren**

*Rector's Office, University of Borås, Borås, Sweden*

<b>1 Introduction</b>	<b>1</b>
<b>2 Physical Principles</b>	<b>2</b>
2.1 Interactions of X-rays with Matter	2
2.2 Principles in Quantitative Evaluation of Element Concentration	3
2.3 Interelement Effects	4
2.4 Dependence of Detection Limits and Penetration Depth on X-ray Energy and Source Characteristics	5
<b>3 Energy-Dispersive X-ray Fluorescence Instrumentation</b>	<b>6</b>
3.1 General Features	6
3.2 X-ray Sources	6
3.3 Energy-dispersive X-ray Fluorescence Spectrometer Designs	8
3.4 Detector Characteristics and New Developments	9
3.5 Micro-X-ray Fluorescence	10
3.6 Portable Systems	10
3.7 Combination with Other Techniques	10
<b>4 Sample Handling and Quantification in Practice</b>	<b>10</b>
4.1 Sample Preparation	10
4.2 Quantitative Analysis of Major or/and Trace Constituents	12
4.3 Surface Analysis and Microanalysis	14
<b>5 Conclusions: Needs for Future Developments</b>	<b>14</b>
<b>Acknowledgments</b>	<b>15</b>
<b>Abbreviations and Acronyms</b>	<b>15</b>
<b>Related Articles</b>	<b>15</b>
<b>References</b>	<b>15</b>

*Energy-dispersive X-ray fluorescence (EDXRF) is an analytical method for qualitative as well as quantitative*

*determination of elements in a sample, independent of their chemical form. It is built on the fact that elements that are irradiated with high-energetic X-rays have a certain probability of emitting characteristic X-rays, the energies of which are unique for each element. In the energy-dispersive (ED) systems, the emitted X-rays are detected via their energies. The use of the EDXRF technique has accelerated since the 1960s as a result of the development of liquid nitrogen cooled solid-state detectors, nuclear electronics, and small computers. Nowadays compact light-weight electrically cooled detectors are available, which, together with air-cooled low-power X-ray tubes, are perfectly suited for handheld spectrometers. EDXRF is multielemental and nondestructive and can be applied to large as well as small samples of different composition and character. If conditions are optimized, minimum detection limits can be below the nanogram absolute or micrograms per gram concentration level for small laboratory instruments and into the femtogram or nanograms per milliliter region for more advanced instrumentation (total reflection X-ray fluorescence (TXRF), synchrotron radiation).*

*EDXRF spectrometers exist at many degrees of sophistication, ranging from advanced laboratory instruments to small portable instruments for field observations. They can be designed for analysis of bulk material or for scanning and elemental mapping of small areas. The use of X-ray optics like single or polycapillaries and curved mirrors in Kirkpatrick–Baez geometry lead to X-ray spot sizes of micrometers and below ideally suited for micro-XRF. Mapping with high spatial resolution is thus possible opening investigations down to cell dimension.*

*Typical applications for EDXRF are analysis of agricultural material, medical samples, archaeological and historical objects, painting and fine art objects, and environmental samples such as soil, ores, water, and aerosol particles.*

## 1 INTRODUCTION

EDXRF is an analytical method for qualitative as well as quantitative determination of elements in a sample, independent of their chemical form. It is built on the fact that elements that are irradiated with high-energy X-rays have a certain probability of emitting characteristic X-rays. The energy,  $E$ , of this radiation is uniquely dependent on the element, which emits the characteristic X-rays by Moseley's law,  $E = K(Z - s)^2$ ,<sup>(1)</sup> where  $K$  and  $s$  are constants that vary with the spectral series and  $Z$  is the atomic number of the element. In ED systems, the emitted X-rays are detected by their energies, whereas in wavelength-dispersive X-ray fluorescence (WDXRF) systems, the physical equivalent to energy, the wavelength

of the characteristic photon is measured. This statement can be explained by the simple relation

$$\begin{aligned} E &= h\nu, \lambda \cdot \nu = c > E = hc/\lambda > E(\text{keV}) \\ &= 1.2396/\lambda(\text{nm}) \end{aligned} \quad (1)$$

from which it is seen that the wavelength and energy of the X-rays are reciprocal to each other.

WDXRF utilizes the properties of single crystals to diffract X-rays of a specific wavelength under a specific angle (Bragg's law) and the intensity of the diffracted radiation is counted by a simple radiation counter e.g. Geiger–Muller counter. As characteristic radiation for one element has a fixed well-defined value  $\lambda$  only at specific angles, a high intensity of the refracted radiation is measured. So using a goniometer with the Bragg crystal as the dispersive element in its center and a detector at the circumference, a continuous rotation will result in intensive peaks whenever the condition of Bragg's law

$$2d \sin \theta = n \lambda \quad (2)$$

is fulfilled. Theta  $\theta$  is the refraction angle,  $\lambda$  is the characteristic wavelength, and  $d$  is the distance between lattice planes of the single crystal. By continuous rotation of the detector from 0 to 180°, angle  $2\theta$ , while the crystal is in position  $\theta$ , collects the photons reflected. This sequential measurement leads to a spectrum “intensity versus wavelength” allowing determination of elements and concentration in the sample because the intensity is proportional to the concentration of the respective element.

In the case of EDXRF, the detector crystal, made of lithium-drifted silicon Si(Li) or hyperpure Ge, takes on two tasks together, namely, dispersion according to the energy and counting of the photons of individual energy. This collection process results in a spectrum “intensity versus energy” of the characteristic radiation emitted from the sample. More details about energy-dispersive detectors are presented later. Typical applications for EDXRF are analyses of agricultural material, medical samples, archaeological and historical objects, and environmental samples such as soil, water, and aerosol particles. EDXRF working is simultaneous, multielemental, and nondestructive, and can be applied to small samples (about 0.1 mg). For scanning objects and mapping small areas in a specimen, EDXRF instruments with narrow beams of X-rays can be used.

WDXRF is widely used for routine analysis and several hundred thousand instruments are distributed in steel production, cement industry, geologic sample analysis, worldwide. In scientific research, the high resolution is appreciated allowing precision measurements in cases where the line overlaps represent a problem in EDXRF.

Owing to the heavy weight of the components, there are no portable WD spectrometers available.

The use of the EDXRF technique has accelerated since the 1960s as a result of the development of solid-state detectors, nuclear electronics, and small computers. Today about 14 000 EDXRF spectrometers are in use, many of which belong to research laboratories. This number is rapidly growing because handheld portable spectrometers combining new detector technologies for charge collection and cooling are available. The composition of fine art objects, scrap metals, wall painting, or environmental samples can be analyzed on the spot, within seconds. A vast number of scientific publications exist on the subject of EDXRF and its applications. Authoritative textbooks on the principles and instrumentation for EDXRF are those of Bertin,<sup>(2)</sup> Jenkins et al.,<sup>(1)</sup> Van Grieken and Markowicz,<sup>(3)</sup> and Beckhoff et al.<sup>(4)</sup>

## 2 PHYSICAL PRINCIPLES

### 2.1 Interactions of X-rays with Matter

When a beam of X-rays (originating e.g. from X-ray tubes) impinges on a sample, it will interact with the atoms in the sample by three processes, namely, the photoelectric effect and coherent (Rayleigh) and incoherent (Compton) scattering. For the photoelectric effect to occur, the energy of the impinging photons has to be large enough to create a vacancy in one of the shells of the studied elements. The photoelectric effect may result in emission of characteristic X-rays, but once a vacancy has been created in an inner shell the atom can also de-excite by emission of Auger electrons. The probability that characteristic X-rays will be emitted – and not an Auger electron – varies from one element to another and is described as the *fluorescence yield*. For elements of low atomic number, emission of Auger electrons dominates, whereas emission of characteristic X-rays is more likely for elements of high atomic number. A sketch of the XRF process leading to emission of a characteristic X-ray is shown in Figure 1. On the basis of Moseley's law the wavelength or energy of the emitted radiation is characteristic for the element and thus the element can be identified.

The scattering processes are of two types, incoherent and coherent. The probabilities of both kinds of scattering vary with photon energy and the composition of the sample. The scattered X-rays are an important part of the background radiation on which the characteristic peaks are superimposed. Figure 2 shows a typical X-ray spectrum with characteristic and scattered radiation.

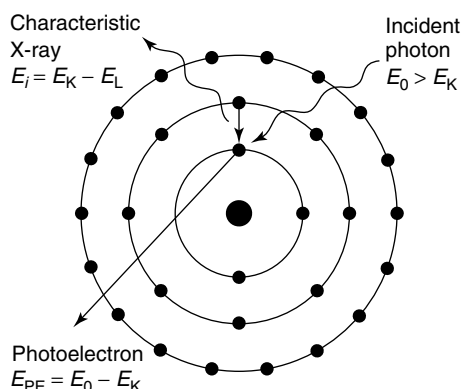


**Figure 1** Schematic drawing of the XRF process in an atom. An incident photon of energy  $E_0$  transfers its energy to an electron in the K-shell. The electron is expelled from the atom and leaves a vacancy. An electron from the L-shell can transit to the K-shell to fill the vacant site. The difference in binding energy between the two shells,  $E_K - E_L$ , is used by the atom to emit a characteristic X-ray of energy  $E$ . Note that the distances between the atomic shells are not drawn to scale but shown schematically only.

## 2.2 Principles in Quantitative Evaluation of Element Concentration

The quantitative evaluation of element concentrations in EDXRF depends on whether the source is

monochromatic or contains a range of different energies. Polychromatic X-ray sources can, however, be treated as a sum (or an integral) of monochromatic sources, and the discussion below is therefore limited to the case of monochromatic excitation. For this case, with further limitations to homogeneous samples and in the absence of interelement effects, a simple relationship can be obtained between the mass thickness (or areal density),  $m_i$ , of a specific element and the measured intensity  $I_i$  of its characteristic X-ray peak:

$$I_i = I_0 K_i m_i D_i \quad (3)$$

where  $I_0$  is the intensity of the primary beam of energy  $E_0$ , which, in the case that the source is a secondary-target X-ray tube arrangement, is influenced by the anode material and operating voltage and current;  $I_i$  is the intensity of characteristic X-rays (K- or L-radiation) of element “ $i$ ” of energy  $E_i$ ;  $D_i$  is a correction factor for attenuation of both the incident X-rays and the characteristic X-rays of element “ $i$ ” in the sample; and  $K_i$  is a factor that depends on the setup of the instrument and basic physical processes.

$K_i$  thus depends on instrumental factors and on fundamental physical parameters related to the energies of the incident and characteristic X-rays. The important parameters to be considered are

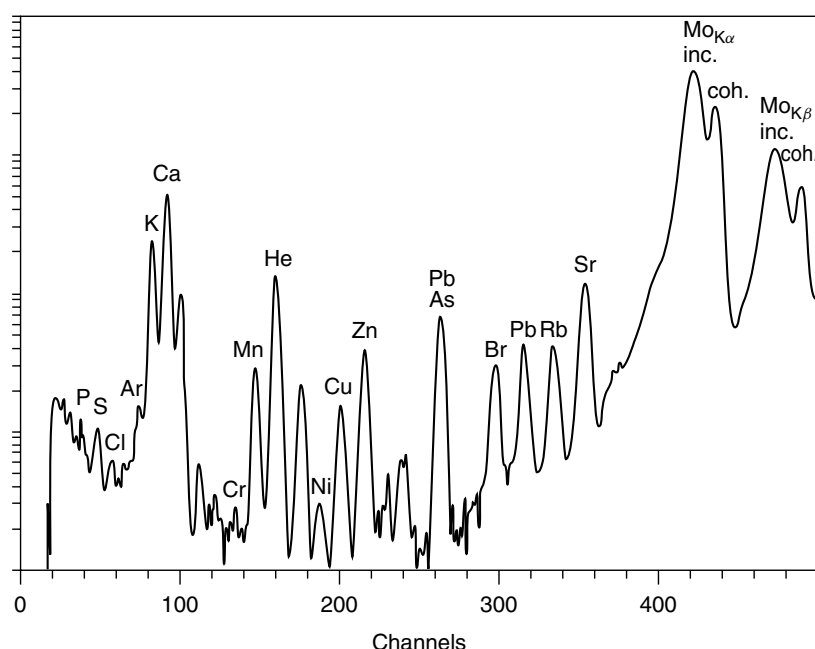


**Figure 2** X-ray spectrum of a biological standard reference material, SRM1571 (National Institute of Standards and Technology (NIST)), “orchard leaves”, measured in a secondary-target EDXRF spectrometer of the geometry of Figure 3. The sample thickness is  $30 \text{ mg cm}^{-2}$ . The excitation conditions were as follows: tube voltage 55 kV and current 10 mA. The characteristic  $K\alpha$  lines are denoted by chemical symbols, except for Pb, for which both  $L\alpha$  and  $L\beta$  are marked. Note the high intensities of the coherently and incoherently scattered  $K\alpha$  and  $K\beta$  radiation of the secondary target, which, in this spectrum, is Mo. The X-ray spectrum has been recorded with an Si(Li) detector.

- the geometry of the XRF spectrometer;
- the attenuation of the exciting and characteristic radiation along the beam paths and in the detector window;
- the detector efficiency for radiation of energy  $E_i$ ;
- the probability of producing a vacancy with incident radiation of energy  $E_0$  in the relevant shell of element “ $i$ ”;
- the fluorescence yield of element “ $i$ ”.

Note, however, that the essential feature of Equation (3) is that – under the assumptions of homogeneity and absence of interelement effects in the sample – the factor  $K_i$  is independent of the mass thickness,  $m_i$ , of the analyzed element and of the attenuation correction,  $D_i$ .  $K_i$  can be determined through calibration of the instrument with suitable calibration standards under well-defined conditions.

The amount of analyte is often written as

$$m_i = W_i m \quad (4)$$

where  $W_i$  is the weight fraction  $m_i$  is the mass thickness of element “ $i$ ” in the sample, and  $m$  is the sample mass.

The attenuation correction,  $D_i$ , in Equation (3) has the form given in Equation (5):

$$D_i = \frac{1 - \exp -[(\mu(E_0) \csc \varphi_1 + \mu(E_i) \csc \varphi_2) \cdot m]}{[\mu(E_0) \csc \varphi_1 + \mu(E_i) \csc \varphi_2] \cdot m} \quad (5)$$

In this expression,  $\mu(E_0)$  and  $\mu(E_i)$  are the mass attenuation coefficients for the exciting and characteristic radiation of energies  $E_0$  and  $E_i$ , respectively; they can be expressed as weighted sums of the individual mass attenuation coefficients for all elements in the sample.  $\varphi_1$  is the glancing angle between the exciting radiation and the sample surface plane and  $\varphi_2$  the glancing angle between the characteristic radiation and the sample surface plane. For two special cases, the attenuation correction and thus Equation (3) simplifies tremendously, namely, for “thin” and “infinitely thick” samples.

In some cases, it is also necessary to take into account the fact that the characteristic radiation produced by an element as well as the scattered radiation can cause fluorescence of another element (interelement and related effects, as discussed below). This effect leads to the enhancement of one spectral line, the absorption already having been taken into consideration. Furthermore, to perform quantitative evaluation, one needs to know whether impurities are present in the spectrometer material and the properties of the detector.<sup>(1–3)</sup>

Equations (3) and (4) require the net peak areas of the characteristic peaks in the X-ray spectrum to determine element concentrations in a sample. This can

be done automatically by means of computer programs. In evaluation of net peak areas in a spectrum, the problem of interference between spectral lines will, however, have to be addressed. In a number of cases, the K-lines from one element will overlap or coincide with the L-lines of another element, as is illustrated in Figure 2 by the overlap of As  $K\alpha$  with Pb  $L\alpha$ . In other cases, the  $K\alpha$  from one element will coincide with the  $K\beta$  from another. By knowing relative ratios,  $K\alpha/K\beta$ ,  $L\alpha/L\beta$ , it is possible to resolve the overlapping peaks. This problem is not so severe in WDXRF as the crystal resolution is in the range of a few electron volts at 5.9 keV, whereas the energy resolution of an ED detector is, for this energy value, at its best around 130 eV at 5.9 keV. However, this procedure of spectrum deconvolution will reduce the precision of the measurement to an extent determined by the statistics of the measurement.

### 2.3 Interelement Effects

In a sample composed of many elements, each element will interact with the radiation from all other elements. If the matrix elements have characteristic radiation that is on the short wavelength side of the absorption edge of the element of interest, element “ $i$ ”, conditions may be favorable for the enhancement of the lines of element “ $i$ ”. The combined effects of the matrix elements on each other are often called *interelement* or *absorption–enhancement* effects. Enhancement effects are especially important for cases in which the analyte is present at trace level and the enhancing elements at percentage levels. In order to illustrate this, consider the determination of one element, “ $i$ ”, by measuring its  $K\alpha$  radiation in a matrix consisting of lighter as well as heavier elements. In this case, the lighter elements will not be able to enhance the characteristic  $K\alpha$  radiation of the element “ $i$ ” because their characteristic radiation will not be energetic enough to create the necessary vacancy in the K-shell of element “ $i$ ” (see Figure 1). Thus, it is necessary to look at the effects of the heavy elements in the sample. If their  $K\alpha$  energies are lower than that of the absorption edge for the K-shell in element “ $i$ ” they will not cause enhancement. If, on the other hand, their  $K\alpha$  lines have higher energies than that of the K-shell absorption edge they will enhance the  $K\alpha$  radiation of element “ $i$ ”. However, the general problem of determining whether or not enhancement will occur is not so difficult for homogeneous samples, since absorption edge energies for different shells and characteristic X-ray energies for all elements are known and readily available in tabulated form in textbooks or from the web.

A situation similar to the interelement effect occurs when the backscattered exciting and/or fluorescent

radiation excites the elements in a thick sample. These effects are of relatively large importance for analysis of trace elements embedded in organic matrices, since the medium-weight and heavy elements are usually present in low concentrations and the incoherent scattering in these cases is dominating.<sup>(5)</sup> (Compare the spectrum from the organic specimen as given in Figure 2.) This fundamental problem described above is the same for EDXRF and WDXRF and must be taken into consideration in both techniques.

#### 2.4 Dependence of Detection Limits and Penetration Depth on X-ray Energy and Source Characteristics

The intensity of a beam of X-rays passing through a sample is attenuated by the above-mentioned photoelectric and scattering processes according to the exponential law:

$$I(E) = I_0(E) \exp(-[\mu(E)\rho x]) \quad (6)$$

where  $I_0(E)$  is the original intensity of the beam;  $I(E)$  is the intensity after the beam has traveled a distance  $x$  in the sample;  $\rho$  is the density of the sample; and  $\mu(E)$  is the mass attenuation coefficient of the sample material. All these considerations are valid for both WDXRF as well as EDXRF.

Since the three attenuation processes that contribute to the total attenuation of the beam are independent of each other, the mass attenuation coefficient can be written as a sum of coherent, incoherent, and photoelectric mass attenuation coefficients. Each process has a functional dependence of the photon energy,  $E$ , shown explicitly in Equation (6).

##### 2.4.1 Penetration Depth

A relevant question in XRF analysis is how deeply the X-rays will penetrate into the material. A quantitative measure of this can be given in terms of the *penetration depth*, which is usually defined as the path length needed for the intensity of the X-rays to be reduced by a given factor. Since the mass attenuation coefficients,  $\mu(E)$ , in Equation (6) vary widely with X-ray energy and material composition, penetration depths are indeed very different for hard and soft X-rays and vary appreciably with sample composition. Table 1 shows some typical values for penetration depths for characteristic X-rays of some elements embedded in an iron and carbon matrix.<sup>(5)</sup> In this example, the penetration depth varies by 3–4 orders of magnitude. Generally, X-rays of low energy do not penetrate very far in a matrix of heavy material, whereas high-energy X-rays in a light material have high penetration. This fact has a large influence

**Table 1** Depth of penetration in micrometers of characteristic radiation from sulfur, chromium, and yttrium in a matrix of iron (density  $7.87 \text{ g cm}^{-3}$ ) and graphite (density  $2.25 \text{ g cm}^{-3}$ ). The penetration depth for reduction of X-ray intensities to two-thirds of the original has been calculated according to the formula  $I = I_0 \exp(-\mu\rho x_{2/3})$ . The elements that generate characteristic radiation are assumed to be present at trace levels, which is why the density of the matrix is not affected

Characteristic radiation	Matrix	Mass attenuation <sup>a</sup> ( $\mu$ , $\text{cm}^2 \text{ g}^{-1}$ )	$x_{2/3}$ ( $\mu\text{m}$ )
SKa	Fe	1170	0.44
CrKa	Fe	119	4.3
Yka	Fe	58.5	8.8
Ska	C	208	8.7
Cr Ka	C	15.3	120
Yka	C	0.813	2200

<sup>a</sup> J.W. Robinson (ed.), *Handbook of Spectroscopy*, CRC Press, Boca Raton, Vol. 1, 1974.

on whether corrections for attenuation have to be made when quantifying element concentrations. Concepts such as “thin or thick” samples are always seen in relation to the energy of the X-rays of interest.

##### 2.4.2 Minimum Detection Limit

A widely used definition for the minimum detection limits (MDL) in EDXRF is the concentration (or, alternatively, the amount of mass) needed for the number of counts in the characteristic peak of an element to be equal to or larger than  $3\sqrt{B}$ , where  $B$  is the number of counts in the background below the peak of the element ( $\sqrt{B}$  corresponds approximately to one standard deviation). Specifically

$$\text{MDL} = \frac{3}{k} \cdot \sqrt{B} \quad (7)$$

where  $k$  is the corresponding sensitivity constant measured as the net number of counts in the characteristic peak per unit concentration and time.

Since the attenuation of X-rays is stronger for soft X-rays than for hard X-rays, the background in many designs of EDXRF spectrometers is rather flat for energies below the scattered radiation. Best values for MDL are usually obtained for medium-weight elements. From Equation (7), it can be seen that the general problem of lowering detection limits can be solved by finding ways of increasing the intensity of the characteristic peak while decreasing the intensity of the background radiation. A substantial portion of the background radiation is due to incoherent and coherent scattering of the primary radiation in the sample itself. These scattered peaks will, by means of secondary processes in the sample, give rise

to a general increase in the background also at lower energies. Furthermore, the scattered radiation will also contribute to an increase in the background level owing to incomplete charge collection and other processes in the solid-state detectors. Therefore, sample properties that influence scattering processes, for example, thickness and average atomic number, have an essential influence on the detection limits in an EDXRF spectrometer.

The counts in both peak and background are time dependent, but in different ways: the peak increases linearly with time, whereas  $\sqrt{B}$  increases with the square root of time. This means that the detection limit will be reduced as analysis time is increased, and the analyst can use this fact if elements present in low concentrations are of special interest. The price paid for improvement in MDL is, of course, a longer running time for the spectrometer. For many laboratory instruments, collection times in the range 200–1000 s for each X-ray spectrum are chosen.

In practice, for bulk samples of organic material, MDLs are of the order of 0.1 ppm for laboratory instruments for monochromatic sources with energy matching the binding energy for the K-shell of the element of interest.<sup>(6)</sup> In bulk geological samples, MDLs are generally somewhat larger. Measured as absolute amounts (for example in mass units), the lowest MDLs can reach the picogram region for thin samples (especially with TXRF<sup>(7)</sup>) and the femtogram region for microbeams that utilize a focused synchrotron beam as source.<sup>(8)</sup>

MDLs in the  $10^{-10}$  g region are reached for many elements in thin and thick samples in laboratory EDXRF spectrometers and MDLs with TXRF yield  $10^{-12}$  g using laboratory sources.

#### 2.4.3 Sensitivity

A concept that is often used to describe the performance of an EDXRF method is the *sensitivity*, which is defined as the change in instrument response (net number of counts in a characteristic peak) per unit change in the concentration of a measured element. Thus, sensitivity in X-ray instruments can be given as count rate per parts per million. The sensitivity concept is useful for comparing analyses of different elements in a given spectrometer. It varies to a high degree with the difference in energy between the incident and the characteristic radiation and is highest if the energy of the incident radiation is only slightly greater than the energy of the K-edge for the element in question.

However, sensitivity in XRF instruments (expressed as count rate per parts per million) is a measure of the excitation and detection capability for each element with a specific XRF instrument. Usually, sensitivity is not used for comparing different instruments but, nevertheless,

is informative. For reasons of comparison, a more appropriate parameter is the MDL achieved with each instrument.

## 3 ENERGY-DISPERSIVE X-RAY FLUORESCENCE INSTRUMENTATION

### 3.1 General Features

A typical feature in element analysis in practice is that samples may contain major as well as trace concentrations of different elements. Samples such as alloys, mineral ores, and ceramics usually contain a number of elements, the concentrations of which may vary by several orders of magnitude.

In an EDXRF spectrometer, the important parts to consider are the X-ray source, the beam and spectrometer geometry, and the detector. An obvious goal for the designer of XRF spectrometers is to maximize the intensity of the characteristic X-rays from the elements while keeping the background radiation as low as possible. Most ED spectrometers have an elemental range from Na to U and, if special detectors with ultrathin windows, polymers of 300 nm supported by a Si grid are used, the range can be extended to still lighter elements such as Be, B, and C.<sup>(9)</sup> There are many different designs of ED spectrometers for laboratory and field work.<sup>(10)</sup> Combinations of WDXRF and EDXRF systems are also used, in which the better resolution of WD instruments is utilized for the lightest elements and the simplicity and higher sensitivity of ED systems is utilized for elements above Ca. The cost of an ED system is about US\$ 70 000 and upward.

### 3.2 X-ray Sources

In photon-induced XRF, the most common sources are X-ray tubes, which can be used directly for broadband excitation or in combination with filters or secondary fluorescers to obtain semimonochromatic radiation. In some spectrometers, especially portable instruments for field work, and for problems in which only one or a few elements are of interest (for example, in routine process control), radioisotopes are still useful.

#### 3.2.1 X-ray Tubes

In X-ray tubes, the radiation spectrum is influenced by two major processes that occur when electrons are accelerated by the high voltage from the cathode to the anode. One process is the creation of characteristic X-rays in the anode material itself, which occurs when the kinetic energy of the impinging electron is larger than

the binding energy of a particular shell in the anode material. The other process is the creation of continuous bremsstrahlung, which is created when the electrons are slowed down in the anode. The bremsstrahlung spectrum contains energies from zero up to the kinetic energy of the electrons, which is equal to the electron charge times the tube voltage. Accordingly, the spectrum from the X-ray tube contains a continuous distribution overlaid with the characteristic radiation from the anode material about 100 times higher in intensity compared to bremsstrahlung in that energy range. By varying parameters such as anode material and thickness, tube voltage, and current settings, the broadband spectrum from the X-ray tube can be optimized for the elements of interest. Some special X-ray tubes are equipped with dual (W/Sc or W/Mo alloy) or multiple anodes mechanically exchangeable in the high vacuum of the tube.

Furthermore, the spot size of the electron focus on the anode material is an important factor defining the emitted brightness. The applicable electric power depends on the size as the heat dissipation is the limiting factor. X-ray tubes with standing anodes have, for Mo and W, typically 3 kW (60 kV and 50 mA) if a focus of about  $0.4 \times 12 \text{ mm}^2$  is used. Broad focus tubes with  $7 \times 7 \text{ mm}^2$  can dissipate up to 40–50 kW. Rotating anodes where the anode is formed like a wheel and rotated at 10 000 rpm allows up to 18 kW for a  $0.5 \times 10 \text{ mm}^2$  electronic focus. Low-power X-ray tubes of 50–75 W (50 kV and 1–1.5 mA) with a focal size of  $100 \mu\text{m} \times 100 \mu\text{m}$  emit a high flux of photons and can be ideally combined with X-ray optical elements to focus the beam to micrometer dimensions with a flux of  $1 \times 10^{10}$  photons/s and are perfect for microanalysis in the lab. These X-ray tubes are air cooled and of light weight, ideally suited for the design of handcarried portable spectrometers.<sup>(11)</sup>

As the MDL for a given element is dependent on the intensity of the characteristic as well as the background radiation (Equation 7), there is often a desire to use monochromatic or quasi-monochromatic radiation. This can be achieved by use of filters and/or secondary-target arrangements. Filters inserted between the X-ray tube and the sample will allow transmission of the characteristic line of the filter but will attenuate the low-energy part of the tube radiation by a substantial factor. Thus, filtering may change the shape of the tube spectrum and improve MDLs for elements lighter than the filter material. By varying filter material and filter thickness, this method can give a high flexibility in the use of tube excitation.

In secondary-target arrangements, the radiation from the X-ray tube is allowed to excite a target made of a material whose characteristic radiation (only the intensive  $K\alpha$  and  $K\beta$  lines are emitted) is used as a source to excite the sample. Figure 3 shows an arrangement of this kind, often called *triaxial geometry* due to the three orthogonal

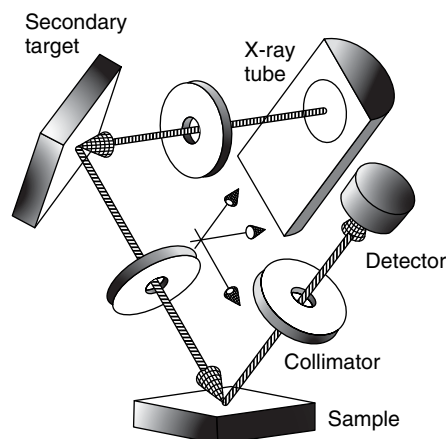


**Figure 3** Preferred geometry of a secondary-target EDXRF spectrometer. The broadband radiation from an X-ray tube excites a secondary target of a pure specimen, most often a metal. The characteristic  $K\alpha$  and  $\beta$  radiation from the secondary target is used as semimonochromatic X-ray source to excite the different elements in the sample. A detector registers the radiation from the sample. Note that the three X-ray beams are mutually orthogonal and that the sample plane is horizontal.

directions of primary beam path, secondary-target beam path, and path from sample to detector. The material in the secondary target can be chosen so that its characteristic radiation is just above the K-edge of the elements of most interest in the sample. The anode material in the X-ray tube is generally chosen to have a high output over a wide range of energies in order to allow different secondary-target materials to be used. Most ideal are combinations where the characteristic radiation from the anode is with its energy just above the absorption edge of the target material e.g. Rh anode–Mo secondary target. Also the tube radiation is linearly polarized after  $90^\circ$  scattering on the secondary target in this orthogonal geometry (all axes have an angle of  $90^\circ$  to each other), thus not contributing to spectral background in the triaxial geometry of Figure 3. Although the intensity of the primary beam is reduced considerably by the secondary-target arrangement, the technique usually gives low detection limits for many elements. This is mainly because of the low background in the X-ray spectra (see Figure 2). Other techniques to modify the output from an X-ray tube utilize low-Z elements (carbon or Plexiglas) scatterers to polarize the entire spectrum of X-rays from the tube or multilayers to obtain an intensive purely monochromatic beam, as demonstrated for TXRF spectrometers (see Strelie et al.<sup>(8)</sup>).

For microbeam EDXRF, microfocus low-power X-ray tubes with anode spots of the order of  $100 \mu\text{m}^2$  are now available, as are high-intensity rotating anode sources (18 kW) with various focal spot sizes (see Beckhoff et al.<sup>(4)</sup>).

### 3.2.2 Radioactive Sources

Radioisotopes as X-ray sources utilize the  $\gamma$ -rays from the decay of the radioisotope or the characteristic X-rays emitted from the decay product. The output intensity is lower than that which can be achieved by an X-ray tube, but the advantages are that the intensity of the source is stable and no electric power supply is needed. Radioisotopes are therefore practicable in portable field instruments. The drawback is the limited half-lives for some of the most commonly used isotopes (for example 2.7 years for  $^{55}\text{Fe}$  with 5.9- and 6.4-keV X-rays (Mn  $K\alpha$  and  $K\beta$  lines) and 1.3 years for  $^{109}\text{Cd}$  with 22.2- and 25.5-keV X-rays (Ag  $K\alpha$  and  $K\beta$  lines) plus 88.2 keV  $\gamma$ -rays). Also  $^{241}\text{Am}$  with 59.5 keV  $\gamma$ -rays is useful for higher- $Z$  element excitation and this isotope has a half-life of 433 years which is convenient. The most common geometries of the radioisotope sources are either that of a point source or that of an annular source. The sensitivity and MDLs are, for some instruments, almost identical to those for X-ray tube secondary-target arrangements.<sup>(12)</sup>

### 3.2.3 Synchrotron Radiation

Synchrotron radiation is the ideal source for EDXRF, since it can be monochromatized to the desired energy with high brilliance. Furthermore, it is linearly polarized in the plane of the electron or positron orbit, which is useful for decreasing scattered radiation and thus reducing the background. Synchrotron radiation at the National Synchrotron Light Source ((NSLS), Brookhaven National Laboratory) with collimated and focused X-rays of high energy has been used in an X-ray microscope, mapping trace elements with a spatial resolution of  $10 \times 10 \mu\text{m}^2$  and with MDLs into the femtogram region for thin specimens.<sup>(13)</sup> However, synchrotron radiation is expensive and is not generally available in research laboratories. TXRF with synchrotron radiation has brought a major breakthrough in the surface analysis of Si wafers at ultratrace levels. Detection limits of absolute 4 fg for Ni corresponding to the more used units in surface contamination of  $5 \times 10^8$  at  $\text{cm}^{-2}$  were achieved in Hamburg at Hasylab Deutsches Elektronensynchrotron (DESY) with monoenergetic synchrotron radiation from a bending magnet beamline.<sup>(14)</sup> Also at Stanford Synchrotron radiation laboratory (SSRL) TXRF measurements were performed showing the low- $Z$  element detection capacity with optimized excitation condition.<sup>(15)</sup>

In a critical review of synchrotron radiation total reflection X-ray fluorescence (SR-TXRF), the advantages and disadvantages can be found in Streltsov et al.<sup>(8)</sup>

Synchrotron radiation is most effective combined with X-ray optical elements like single or polycapillaries or

Kirkpatrick–Baez optics with two mirrors leading to sensational beam dimensions of micrometers and even down to 30 nm. This is ideally suited for elemental analysis of cell material and inclusions in geological formations. Also micro-XRF in human bone, radioactive particles and paintings were reported Janssens et al.<sup>(16)</sup>

## 3.3 Energy-dispersive X-ray Fluorescence Spectrometer Designs

As already pointed out, there are three main points to consider for achieving good performance in an EDXRF system, namely the X-ray source, the detector, and the design of the spectrometer. A few things of importance for the design are mentioned here, namely, beam geometry, choice of materials, and compactness of the design.

The problems are discussed from the perspective of a secondary-target setup but are easy to generalize for other arrangements.

### 3.3.1 Beam Geometry

A large part of the background signals in X-ray spectra depends on primary and secondary scattered radiation in the sample. This can be illustrated in the secondary-target XRF arrangement shown in Figure 3. In such a system, contributions to the background in the final spectrum are obtained from (i) the scattered primary radiation from the tube; (ii) the scattering of the quasi-monochromatic beam from the secondary target; (iii) the radiation from the sample; (iv) detector artifacts like tailing stemming from incomplete charge collection; (v) escape and sum peaks; and (vi) Compton backscattering from high-energy photons leading to high background in the lower energy region. Instrumental blank spectrum from collimators can be a problem in the detection of ultratrace elements if the instrument lines are the same as in the analyzed sample.

The primary radiation from the X-ray tube is very intense and, although it will be scattered twice (in the secondary target and the sample), it is likely to contribute to the background unless special care is taken. The radiation from the secondary target will be scattered upon reaching the sample and constitutes the four large scattered peaks shown in Figure 2. These peaks have been observed to be responsible for part of the flat background in the low-energy region by multiple scattering in the sample and by incomplete charge collection effects in the detector.

From basic physical principles, it is well known that scattering is at a minimum when the scattering angle is  $90^\circ$ . Thus, it is important that the impinging and emitted radiation form an angle of  $90^\circ$  with respect to each other. This will be achieved if the secondary target and the sample are both oriented at angles of incidence of  $45^\circ$  with

respect to the beam directions. Because the radiation from the X-ray tube is scattered twice – in the secondary target and in the sample – and since the reason for scattering at  $90^\circ$  is to utilize both minimum scattering cross section and the production of a linearly polarized beam, it is also of importance that the geometry of the three beam paths is a triaxial ( $xyz$ ) geometry as shown in Figure 3 and not an  $xyx$  planar geometry.<sup>(17)</sup>

### 3.3.2 Choice of Materials – Compact Designs

In an EDXRF spectrometer, the major part of the primary radiation emitted by the tube and secondary target will not only be directed toward the sample but will also interact with the spectrometer. This interaction will take place by means of the same processes as in the sample itself. Different materials have different abilities to scatter and absorb radiation, and the purity of the material will have an influence on whether characteristic lines from impurities in the material close to the beam paths will pass into the detector. Thus, it is important that the materials in objects such as filters and collimators are of the highest possible purity.

Another important aspect to consider in an XRF setup are the actual geometric dimensions of the various parts of the spectrometer. Since the general goal is to have efficient and high sensitivity in the instrument, long beam paths are of disadvantage. In air, a long beam path for the radiation from sample to detector will contribute to the attenuation of characteristic radiation from the sample, and thus significantly reduce detection efficiency for light elements in particular. Thus, a geometry as compact as possible with short beam paths is desirable. However, the material in the housing of the spectrometer has to be chosen so that unwanted radiation can be stopped efficiently. The combination of compact geometry and high stopping efficiency generally means that light materials such as aluminum should be avoided or that the radiation channels have to be clad with higher- $Z$  materials having good absorption properties.

Another aspect to consider in relation to Figure 3 is the position of the sample. In many spectrometers, the sample position is vertical, which means that samples have to be self-supporting. By choosing an arrangement in which the sample plane is horizontal and the detector looks down or up at the sample, a more versatile instrument is achieved, in which the sample can also be in nonself-supporting forms, for example, as liquids and powders. With a vertical sample position, such specimens are difficult to irradiate directly by the beam. Measurements of light elements require a special environment – either vacuum or He flushing – to avoid absorption of the low energy radiation. Thus vacuum chambers holding all components of the spectrometer, in particular, sample and detector

snout inside, are designed for this purpose. In combination with special detectors having ultrathin windows, elements from Be upward can be detected. To evacuate the sample area comprises two other advantages: the scatter of the exciting radiation in air is avoided, which improves the scattered background, and the Ar K-lines will not be measured since Ar is not present in vacuum.

### 3.4 Detector Characteristics and New Developments

For ED spectrometers, liquid-nitrogen-cooled Si(Li) detectors are the most widely used, having their performance for X-rays of an energy ranging from 1 to about 25 keV and described by the efficiency of the detector. For K-lines from heavier elements (30–100 keV) the planar high-purity germanium detectors are preferable owing to their better detection efficiency in this region; the formerly available Ge(Li) is not produced any longer. The classical LN<sub>2</sub>-cooled detector is bulky because of the storage vessel (Dewar) for the cooling medium. An elegant way to get rid of the Dewar is the use of electrical cooling by Peltier elements. These Peltier-cooled detectors operate not at 77 K but around 240 K, which is reached by one- or two-stage Peltier elements working with a power of 3–4 V and 1–2 A.

The fundamental working principle of an ED detector is the absorption of the characteristic photons in the intrinsic zone of the Si crystal. The energy absorbed in the semiconductor material creates a certain number of electron–hole pairs, linearly correlated to the energy of the photons. These charges, created in the intrinsic zone of the Si crystal, form a charge pulse collected at the respective electrodes on the contact layers across the surface of the Si crystal and are proportional to the energy of the absorbed photon. This p–i–n (positive–intrinsic–negative)-type structure of the Si detector collects the charges along the parallel electric field lines between p- and n- silicon and the contact layers under reverse high voltage. A new idea to change the way of collecting charges is the sideward drift.<sup>(18)</sup> In this case, the positive electron-collecting electrode is small and located either at the center of the crystal or slightly eccentric at the outside of the detector structure, and has the electric field lines parallel to the surface of the detector crystal. According to the collection mode, these detectors are termed *drift detectors*. The advantage is high energy resolution, high throughput, and operation at 220–250 K. The charge cloud is collected by a charge-sensitive preamplifier and transformed into a voltage signal that is amplified through the classical electronic amplification chain of preamplifier and amplifier/shaper, and converted from the analog signal into a digital one by the ADC (analog-to-digital converter). Modern electronics use direct conversion and digitize the preamp

signal immediately (DSP (digital signal processing)) leading to best possible energy resolution in the range of 125–130 eV at 5.9 keV, which is the accepted reference energy emitted from a  $^{55}\text{Fe}$  source. Another new feature of a modern ED detector is the extension of the detectable range of elements to the light elements like Be, B, C, N, O, F, Na, Mg, and Al. This is possible because, instead of the Be entrance window, polymer structures of 300-nm thickness supported by a Si grid (Moxtek window trade mark (TM)) can withstand air pressure and are not absorbing as strongly as 8- $\mu\text{m}$  Be which normally is in use. Also, the contact layers on the crystal are extremely thin giving an adequate efficiency in the energy region of the light elements. All measurements for light elements have to be performed in vacuum to avoid absorption of the fluorescence radiation on the path to the detector. The dimensions of pin-type detectors range from 10 to 100 mm<sup>2</sup> with a thickness of 3–4 mm, the silicon drift detectors (SDD) have typically 10–100 mm<sup>2</sup> area but are between 300 and 500  $\mu\text{m}$  in thickness. As a result of the thinner crystal dimension, a poorer efficiency of the SDD is observed. It continuously drops from about 10 keV compared to the Si pin where the decrease of the efficiency starts roughly at 20 keV. For benchtop and portable spectrometers, scintillation counters and gas-filled proportional counters are sometimes used, often in combination with filters to compensate for the lack of energy resolution. Other types of detectors have been developed, for example, mercury iodide detectors at room temperature for high- and medium-*Z*-element analysis.<sup>(19)</sup>

High-purity Si detectors are now able to separate K fluorescence lines down into the 1-keV region and compare well with compound semiconductor detectors such as CdZnTe and HgI<sub>2</sub>.<sup>(20)</sup> An overview of the present status of several semiconductor detectors can be found in the article by McGregor and Hermon,<sup>(21)</sup> and Beckhoff et al.<sup>(4)</sup>

Arrays of SiLi, GeHP, or SDD are available with up to 100 elements, increasing the solid angle of detection drastically – obviously extremely expensive instruments.<sup>(22)</sup>

### 3.5 Micro-X-ray Fluorescence

The use of X-ray optical elements such as single or polycapillaries, where X-ray total reflection occurs on the inner wall side in of a thin-walled tube, on the inner wall side X-ray total reflection occurs is leading to a focussed beam of high intensity. A bunch of several hundred thousands of single capillaries form the polycapillary with intensities several orders of magnitude higher than a pinhole of the same dimension. Scanning in steps of micrometers according to the spot dimensions allows high

spatial resolution mapping. In a particularly interesting geometry, placing a second polycapillary in front of the detector and aligning the system to have both foci matching on the surface of the sample where the X-ray beam impinges, leads to the so-called confocal geometry with the possibility to scan layer by layer starting from the surface and getting a 3D image at the end. Even absorption effects can be corrected as the depth is well known. A typical voxel size is  $20 \times 20 \times 20 \mu\text{m}^3$ . Since the spectra in each measured position is known, an elemental presentation in 3D is finally possible (chemical imaging).<sup>(23)</sup>

An excellent review of microanalysis is given in Ref. 16. Figure 4 shows an example of 2D imaging of a bone sample.

### 3.6 Portable Systems

Developments in excitation sources, detectors, and micro-processor technology have facilitated the design of ED configurations capable of analyzing most elements with detection limits below the milligram per kilogram level. In the last 20 years, portable XRF systems have also been developed and are now commercially available, making it possible to take the spectrometer to the sample rather than the other way round. A detailed review has been published by West and Potts.<sup>(24)</sup>

Special applications find the portable systems in the field of archaeometry and cultural heritage investigations as the technique is nondestructive. Further in-field measurements and screening of hazardous substances are possible with handheld systems.

### 3.7 Combination with Other Techniques

A comprehensive review on recent technological advances is given by Tsuji et al. in Tsuji et al.<sup>(25)</sup>

## 4 SAMPLE HANDLING AND QUANTIFICATION IN PRACTICE

### 4.1 Sample Preparation

A typical feature in element analysis in practice is that samples may contain high as well as trace concentrations of different elements. Samples such as alloys, mineral ores, and ceramics usually contain a number of elements whose concentrations may vary by several orders of magnitude.

EDXRF analysis can be performed on a vast number of samples of very different composition and status. Examples of common samples are

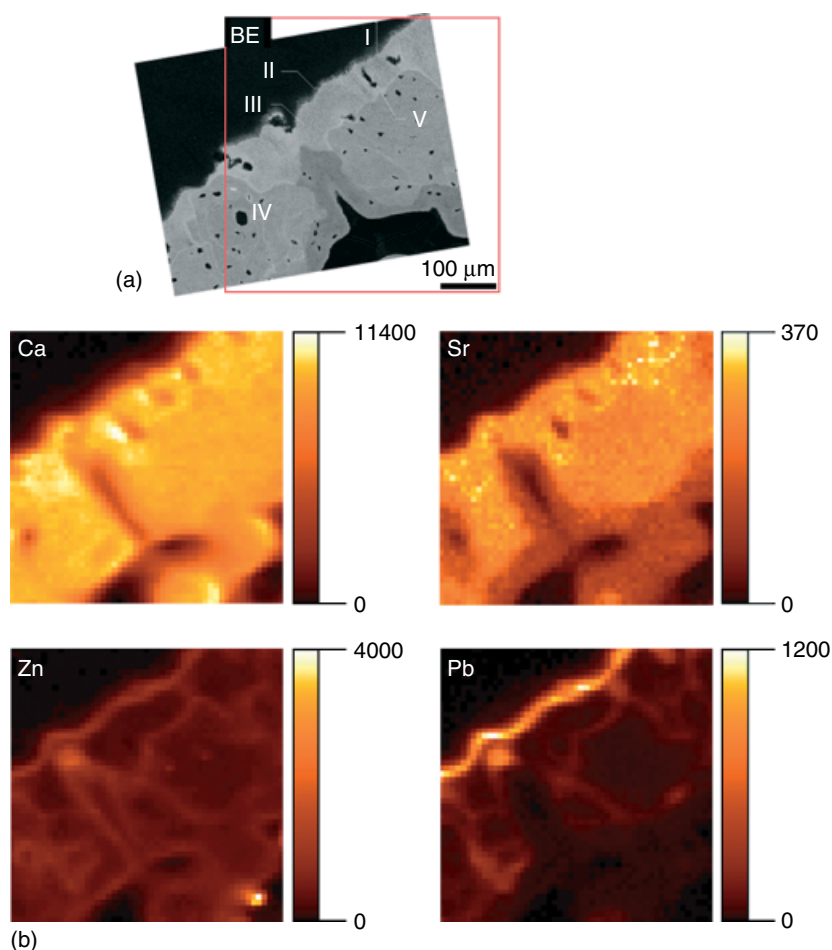


**Figure 4** Elemental (Ca, Sr, Zn, and Pb) 2D image of a bone sample.

- geological – for example minerals, rock, soil, and sediments;
- biological – roots, leaves, stems, moss, lichens, algae, fish, and animals;
- medical – blood, hair, skin, muscle, brain, teeth, bone, enzymes, and metalloproteins;
- industrial – metals, ores, paper, and pulp;
- cultural – pottery, paintings, statues, coins, books, and clothes;
- environmental – water, air pollutants, waste, and pollen;
- pharmaceuticals;
- food stuff and drinking water, wine, or brandy.

There is no strict division between the different categories, but the above list gives an idea of the diversity of the samples concerning range of elemental concentrations – from traces in biological material to major components in minerals – as well as the range of densities involved. The material may exist in different forms, such as airborne particles, liquids, and solids.

#### 4.1.1 Solid Samples

Homogeneous samples for which the concentrations of the elements of interest are significantly larger than the detection limits (usually 0.1–1 ppm) are conveniently analyzed without any sample preparation. This is a great advantage, since a minimum of sample treatment will minimize the risk of contamination. Many samples belong to this category.

Some samples may have sufficiently high element concentrations but may be inhomogeneous and contain grains of different sizes. In view of the poor penetration depths for X-rays from light elements, the grain size may affect the quantitative evaluation. For such samples, either grinding into a fine powder or digestion and dilution may be necessary.

#### 4.1.2 Liquid Samples

Trace elements in water samples can be present in different forms, for example as insoluble particulates or as colloidal or soluble species. Suspended material can be

separated by filtration, and the deposits on the filter can be directly analyzed in the X-ray spectrometer. For water, many element concentrations are below MDLs, especially for heavy metals. The colloidal and soluble fractions may therefore need preconcentration, which may be achieved by evaporation by heating or by freeze-drying. Care must be taken, however, to avoid loss of volatile elements in these processes. A freeze-dried residue may be acid-digested. A number of other chemical preconcentration procedures have been used on natural waters, snow, and rain, with acceptable precision and recovery rates.<sup>(26)</sup> Many of these techniques have the advantage that they increase element concentrations, and at the same time, giving rise to thin film samples that are easy to evaluate quantitatively. For many fluids – and in particular if the TXRF technique is used – the fluid can be deposited directly onto a carrier and dried at low temperature. TXRF shows excellent results for the analysis of Pb, Hg in water where  $10 \mu\text{g L}^{-1}$  MDL can be reached.

Details on sample preparation are given in **Sample Preparation For X-Ray Fluorescence Analysis**

## 4.2 Quantitative Analysis of Major or/and Trace Constituents

As discussed in Section 3.2, quantification involves knowledge of some factors that are different for each spectrometer (geometrical properties, detector and source characteristics, etc.) and some parameters that are dependent on physical processes. In a practical case, both these aspects have to be taken into account.

### 4.2.1 Homogeneous Samples: General Approach

Samples analyzed in spectrometers with monochromatic or nearly monochromatic X-ray sources are usually rather easy to work with, since Equations (3–5) and (6–8) can be used for quantitative evaluation. A convenient approach is to calibrate the spectrometer with known standards, which are either thin or of known mass thickness. Calibration thus gives information on the factors  $K_i$  for different characteristic X-ray energies, for a certain element. These factors can be stored for a special configuration of a given spectrometer and used for element quantification of the unknown samples. If an unknown sample is considered to be thin for some elements ( $D_i = 1$ ), the amounts of these elements can be readily evaluated by using Equation (3). If the sample is of intermediate or infinite thickness, the attenuation factors  $D_i$  will have to be evaluated either from measurements of mass thickness or from information contained in the coherently and incoherently scattered radiation, as discussed below.

For polychromatic X-ray sources, for example broad-band excitation from X-ray tubes, Equation (3) is not valid. In this case, the intensity,  $I_i$ , can be described by an integral over the distribution of excitation energies. In practice, the approach often used is to calibrate the instrument with standards as similar as possible to the investigated samples.

Liquids are a special case of homogeneous samples. For most liquid samples, quantification is facilitated by the ability to spike the sample with internal standards before digestion or further treatment. By choosing two internal standards with different attenuation properties, the attenuation for all elements in the sample can be obtained together with information on the sample mass thickness. In TXRF, samples are prepared on a reflector as thin films achieved after the drying process of the liquid solution where the addition of one internal standard was done. The quantification is easily done with reference to this internal standard added to the solution, using the calibration data for each element expressed as sensitivities achieved from a set of multielement standards with varying concentrations. The equation reads as follows:

$$C_x = I_x/S_x \times S_{\text{std}}/I_{\text{std}} \times C_{\text{std}} \quad (8)$$

where  $C_x$  denotes concentration of the unknown;  $I_x$ , the intensity of the unknown element;  $I_{\text{std}}$ , the intensity of the standard;  $S_x$ , the sensitivity of unknown element;  $S_{\text{std}}$ , the sensitivity of standard; and  $C_{\text{std}}$ , the concentration of standard.

In this case, after the calibration of the spectrometer is established, the sample is spiked with the known amount of internal standard and dried on a reflector serving as sample carrier, and after EDXRF analysis, the evaluation of the intensities will lead immediately to quantitative results of the unknown elements in the sample.

### 4.2.2 Heterogeneous Samples

For heterogeneous samples, quantitative evaluation is more difficult, and this is particularly the case for X-rays from light elements, for which the penetration depths of the characteristic X-rays are small. Another problem with heterogeneous samples is the profile of the X-ray beam itself. In the ideal case, the beam intensity should be constant over the beam area and drop abruptly to zero at the edges of the beam. In reality, the beam intensity does not behave so well, at least not for the radiation from X-ray tubes. Owing to the geometrical effects and different path lengths for different parts of the radiation from the tube to the sample, the beam may not have a homogeneous intensity distribution. This has also been shown to be the case for secondary-target arrangements.<sup>(27)</sup> Thus, for laboratory instruments,

knowledge of intensity variations within the beam is essential for heterogeneous samples. Alternatively, one can achieve good accuracy for heterogeneous samples and beams by scanning the sample, so that effects due to sample and beam inhomogeneity can be leveled out.

#### 4.2.3 Methods for Quantification in Practice

Many samples can be regarded as “thin” for medium- and high- $Z$  elements, but in reality, few samples are thin with respect to light elements of low atomic number  $Z$  (see Table 1). Thus, one will often have to evaluate the attenuation properties of the sample, at least for some elements. Many methods have been developed to assist quantification. Some of these use an experimental approach, whereas others build on the fundamental parameters of the physical processes involved, often in combination with knowledge after calibration of the instrumental performance. A few methods to illustrate the principles in quantitative evaluations for nonliquid samples are described.

The first method, which was one of the earliest, is the emission–transmission method.<sup>(1,2)</sup> A precondition is that the sample is of “intermediate thickness”, meaning that the intensity of the characteristic X-rays grows with sample thickness, but it does not grow linearly. The method is based on an independent measurement of the factor  $\exp[(\mu(E_0) \csc \varphi_1 + \mu(E_i) \csc \varphi_2)m]$ , which is contained in the attenuation correction,  $D_i$ . This factor, which measures the sample attenuation, can be directly evaluated from three measurements:

1. First the characteristic radiation from an element “ $i$ ” in the sample is measured.
2. Under identical conditions, the same characteristic radiation is measured from the combination of the sample and a target of element “ $i$ ” positioned behind the sample.
3. In the third measurement, the characteristic radiation is measured from the target of element “ $i$ ” alone, without the sample.

It is not difficult to show that these measurements will give knowledge of the factor  $\exp[(\mu(E_0) \csc \varphi_1 + \mu(E_i) \csc \varphi_2)m]$ , which is needed in Equation (5). If this factor is known, it is straightforward to calculate  $m_i$  of element “ $i$ ” from measurement of  $I_i$  and knowledge of the instrumental factors  $K_i$  and  $I_0$  according to Equation (3).

Another well-known method is to make use of the information contained in the coherent and incoherent scattering of the incident (exciting) radiation. Under certain conditions, the intensity of the scattering peaks or combinations of these can be used as internal standards.<sup>(1,2,19–21)</sup> From Figure 2, which is an X-ray

spectrum from a biological sample, in which Mo has been used as secondary target, it is seen that the incoherently scattered radiation is very pronounced. In a biological or other kind of light-element sample in which medium and heavy elements are present at trace levels, the incoherently scattered radiation is essentially a measure of the mass seen by the impinging beam. The argument for this is that for the light elements (except hydrogen), e.g. carbon, nitrogen, and oxygen, which are the main constituents in most biological samples, the mass of an atom is closely proportional to its atomic number ( $Z$ ).

Furthermore, the binding energies of the electrons in the light elements are small compared with the energy of the exciting radiation. Thus, the exciting radiation essentially sees a cloud of free electrons, and the probability of incoherent (Compton) scattering will be proportional to the number of electrons, which, in turn, is approximately proportional to the sample mass. This approach is also valid for some elements of importance in geochemical samples, such as Mg, Si, and Ca (ratios of relative atomic mass to atomic number: 2.03, 2.01, 2.00) but less so for Na, Al, and K (ratios of whose relative atomic mass to atomic number are in the range 2.09–2.06). For samples composed of heavy elements, the ratios of atomic mass to atomic number will change owing to increased neutron excess in the atomic nuclei. Furthermore, the binding energy of the inner electrons increases and the free electron incoherent scattering cross section is no longer such a good approximation. Secondary scattering effects in the material may also appear. Several practical methods, however, have been developed, which make use of the information contained in both coherently and incoherently scattered radiation for thick samples of geochemical origin. Giauque et al.<sup>(28)</sup> and Giauque<sup>(29)</sup> have used the ratios of the incoherently scattered radiation from Ag  $K\alpha$  and  $K\beta$  radiation together with the coherently scattered Ag  $K\alpha$  to ascertain sample mass thickness and photoelectric cross sections for thick geochemical samples. Also, in the case of WDXRF, the scattered Compton lines from the X-ray tube have proved to be useful as internal standards in light-element samples.<sup>(30)</sup>

The general aim of quantification in EDXRF is to arrive at the sample composition from the information contained in the spectrum. In an XRF spectrum, the medium-heavy and heavy elements in the sample will reveal their presence by their characteristic radiation as well as by their contribution to the coherently and incoherently scattered radiation. Thus, a first estimate of the relative abundance of these elements can be made directly from the spectrum. As discussed earlier, however, this first estimate will be significantly modified by considering attenuation and interelement effects, etc. To evaluate the mass thickness of the light elements – which

do not show up by their characteristic X-rays – their contribution to the scattering peaks can be determined from the spectrum by subtraction of the scattering due to the medium-heavy and heavy elements. From this evaluation, the total mass thickness from light as well as medium and heavy elements can be calculated.

In an iterative process, in which all the information from the elements through their characteristic as well as scattered X-rays is used, the concentrations can be recalculated until the concentration values obtained agree with the experimental spectrum.

In the practical situation, the analyst is dependent on computer programs in which an X-ray library is stored together with information on the actual spectrometer (obtained by calibration samples). Spectrum evaluation programs are available in commercial instruments and from research groups. A more-or-less continuous development of these programs takes place, in which peak shapes and background profiles are described by model functions.<sup>(31)</sup>

#### 4.3 Surface Analysis and Microanalysis

Quantification of thin surface layers or microstructures essentially makes use of the same fundamental methods as discussed above, namely, adding of an internal standard for liquids, use of external reference material, and use of scattered radiation. For thin self-supporting homogeneous solid surface layers, quantification can be achieved by use of scattered radiation, calibration constants, or fundamental parameters.

In microelectronics, layers and implants need to be prepared in the nanometer region. In these cases, the Si wafer, as the basic material, is the best substrate for TXRF in order to use the angle-dependent fluorescence signal of the layer or implant to derive information on layer thickness, element and density – in case of implants the concentration profile can be derived by angle scanning from 0° to 2–3 times the critical angle. This technique is sensitive in the nanometer range and allows excellent insight to the new design of ultrashallow junctions. Both, laboratory sources and synchrotron radiation can be used for these applications, called *grazing incident X-ray fluorescence (GIXRF)*.<sup>(32)</sup>

In the case of heterogeneous microstructures smaller than the X-ray beam diameter, quantification by means of external references is difficult in spectrometers based on X-ray tubes owing to the inhomogeneous beam profile as discussed above, and the difficulty in positioning the samples within the beam. In these cases, internal standards such as the scattering peaks from the sample will give reasonably good average values, although structures with resolution below 10 μm are presently difficult to study with laboratory equipment.<sup>(33)</sup>

## 5 CONCLUSIONS: NEEDS FOR FUTURE DEVELOPMENTS

Although EDXRF has many advantages, in that it is multielemental, nondestructive, and needs a minimum amount of sample treatment, it has two distinct disadvantages:

- For bulk samples it is not very sensitive. MDLs for laboratory equipment are in the order of 0.1 ppm. Measured in mass units, it has MDLs of the order of a fraction of a nanogram for the best cases in realistic samples. For synchrotron radiation sources and special designs (TXRF; grazing emission X-ray fluorescence (GEXRF)), MDLs may be reduced by several orders of magnitude, but not for all kinds of samples. A substantial part of the lack of sensitivity for bulk samples is due to effects caused by the presence of the large scattered peaks entering the solid-state detectors.
- In comparison with microprobes with charged particles – electrons or protons – microprobes of X-rays with high lateral resolution are difficult to obtain. This is because charged particles can be steered by electric and magnetic fields, whereas X-rays will have to be focused with mirrors or other kinds of optical devices. The advantage of X-rays over charged particles is that they deposit less energy into the sample and thus will cause less heating and loss of volatile material.

Within a few years, EDXRF has mutated into a very versatile analytical tool owing to the development of sources, optics, and detectors. The applicability of EDXRF has been drastically enhanced in various fields. Quantification is no longer a big problem since the knowledge of primary X-ray spectra and fundamental parameters has drastically improved. The improvement in computing capability and speed has led to faster quantification and data evaluation. Software packages are available as freeware, performing spectrum deconvolution to obtain net counts for each element of the sample and also solving the rather complicated equations related to all interaction processes rapidly in seconds.

The elemental mapping capacity (2D and 3D) with high power sources opens new applications in medicine, biology, environment, and cultural heritage investigations, where quantification is not the most relevant information.

EDXRF has reached a degree of maturity with regard to accuracy and precision of the measurements. New sources – X-ray optics and various excitation geometries, like TXRF, GIXRF, and GEXRF – have shown a wide field of applications in layer and implant characterization. In combination with high-resolution single crystals

in double-crystal arrangements, energy increments of 100 meV are possible; this can be used to study the chemical state by measuring the fluorescence signal in dependence of the incident photon energy around the absorption edge of the element considered. X-ray absorption near edge spectroscopy (XANES) is used to determine the chemical state of the element, extended X-ray absorption fine structure (EXAFS) is used to determine the coordination number and the distance to the neighboring atoms.

Further developments of X-ray sources like free electron lasers X-ray free electron laser (XFEL) and Linac coherent light source (LCLS) will be soon available for the scientific community and will require the development of ultrafast detector technology and electronics to make use of the high brilliant sources for EDXRS.

Future development, which would imply breakthroughs on the above items, would be

- improvements in detector technology to minimize effects that cause increased background, for instance trapping and polarization in the detector material;
- development of laboratory X-ray lasers in order to obtain parallel, polarized, and intense beams.

For both these developments it is easy to observe that not only EDXRF but also a vast field of other analytical methods would benefit from them.

## ACKNOWLEDGMENTS

One of the authors, E. Selin Lindgren, is grateful to Ing. Paulis Standzenieks for assistance in preparing the manuscript.

## ABBREVIATIONS AND ACRONYMS

ADC	Analog-to-Digital Converter
DESY	Deutsches Elektronensynchrotron
DSP	Digital Signal Processing
EDXRF	Energy-Dispersive X-ray Fluorescence
ED	Energy-Dispersive
EXAFS	Extended X-ray Absorption Fine Structure
GEXRF	Grazing Emission X-ray Fluorescence
GIXRF	Grazing Incident X-ray Fluorescence
LCLS	Linac Coherent Light Source
MDL	Minimum Detection Limits
NIST	National Institute of Standards and Technology
NLSL	National Synchrotron Light Source

p-i-n	Positive-Intrinsic-Negative
SDD	Silicon Drift Detectors
SR-TXRF	Synchrotron Radiation Total Reflection X-ray Fluorescence
SSRL	Stanford Synchrotron Radiation Laboratory
TM	Trade Mark
TXRF	Total Reflection X-ray Fluorescence
WDXRF	Wavelength-Dispersive X-ray Fluorescence
XANES	X-ray Absorption Near Edge Spectroscopy
XFEL	X-ray Free Electron Laser

## RELATED ARTICLES

*Environment: Water and Waste (Volume 4)*  
Sample Preparation for Elemental Analysis of Biological Samples in the Environment • X-ray Fluorescence Spectroscopic Analysis of Liquid Environmental Samples

*Forensic Science (Volume 5)*  
X-ray Fluorescence in Forensic Science

*Peptides and Proteins (Volume 7)*  
X-ray Crystallography of Biological Macromolecules

*Steel and Related Materials (Volume 10)*  
X-ray Fluorescence Spectrometry in the Iron and Steel Industry

*Nuclear Methods (Volume 14)*  
Particle-induced X-ray Emission (PIXE)

*Radiochemical Methods (Volume 14)*  
Nuclear Detection Methods and Instrumentation

*X-ray Spectrometry (Volume 15)*  
Portable and Handheld Systems for Energy-dispersive X-ray Fluorescence Analysis • X-Ray Fluorescence Analysis, Sample Preparation For • Total Reflection X-ray Fluorescence • Wavelength-dispersive X-ray Fluorescence Analysis • X-ray Techniques: Overview

## REFERENCES

1. R. Jenkins, R.W. Gould, D. Gedcke, *Quantitative X-ray Spectrometry*, Marcel Dekker, New York, 1981.
2. E.P. Bertin, *Principles and Practise of X-ray Spectrometric Analysis*, Plenum Press, New York, 1975.

3. R.E. Van Grieken, A.A. Markowics (eds), *Handbook of X-ray Spectrometry*, 2nd edition, Marcel Dekker, New York, 2002.
4. B. Beckhoff, B. Kanngießer, N. Langhoff, R. Wedell, H. Wolff (eds), *Handbook of practical X-ray Fluorescence analysis*, Springer, Berlin, Heidelberg, New York, 2006.
5. A.G. Karydas, T. Paradellis, 'Calculation of the Enhancement of Characteristic Radiation Due to Scattering in Radioisotope XRF Using Exact Differential Cross-sections', *X-ray Spectrom.*, **22**(4), 208–215 (1993).
6. R.P. Pettersson, E. Selin Lindgren, 'Energy-dispersive X-ray Fluorescence Analysis', in *Surface Characterization, A User's Sourcebook*, eds. D. Brune, R. Hellborg, H.J. Whitlow, O. Hunderi, Wiley-VCH, Weinheim, 136–153, 1997.
7. P. Wobrauschek, Total reflection x-ray fluorescence analysis – a review, *X-ray Spectrom.*, **36**, 289–300 (2007).
8. C. Strelis, P. Wobrauschek, F. Meirer, G. Pepponi, Total reflection X-ray fluorescence and grazing incidence X-ray spectrometry – Tools for micro- and surface analysis. A review, *J. Anal. Atom. Spectr.*, **23**, 792–798 (2008).
9. www.moxtek.com, 2009.
10. www.panalytical.com, www.rigaku.com, www.spectro.com, www.edax.com, www.oxford-instruments.com, www.thermofisher.com, 2009.
11. homepage of oxford instruments: www.oxfordxtg.com, 2009.
12. V. Valkovic, A. Markowics, N. Haselberger, 'Review of Recent Applications of Radioisotope Excited X-ray Fluorescence', *X-ray Spectrom.*, **22**(4), 199–207 (1993).
13. K.W. Jones, W.M. Kwiatek, B.M. Gordon, A.L. Han-son, J.G. Pounds, M.L. Rivers, S.R. Sutton, A.C. Thompson, J.H. Underwood, R.D. Giaque, Y. Wu, 'X-ray Microscopy Using Collimated and Focussed Synchrotron Radiation', *Adv. X-ray Anal.*, **31**, 59–68 (1987).
14. C. Strelis, G. Pepponi, P. Wobrauschek, C. Jokubonis, G. Falkenberg, G. Zaray, J. Broekaert, U. Fittschen, B. Peschel, Recent results of synchrotron radiation induced total reflection X-ray fluorescence analysis at HASYLAB Beamline L, *Spectrochim. Acta*, **61B**, 1129–1134 (2006).
15. C. Strelis, G. Pepponi, P. Wobrauschek, N. Zöger, P. Pianetta, K. Baur, S. Pahlke, L. Fabry, C. Mantler, B. Kanngiesser, W. Malzer, Analysis of low Z elements on Si wafer surfaces with synchrotron radiation induced total reflection X-ray fluorescence at SSRL, Beamline 3–3: comparison of droplets with spin coated wafers, *Spectrochim. Acta*, **58B**, 2105–2112 (2003).
16. K. Janssens, F. Adams, A. Rindby (eds), *Microscopic X-ray Fluorescence Analysis*, Wiley, 2000.
17. P. Standzenieks, E. Selin, 'Background Reduction of X-ray Fluorescence Spectra in a Secondary Target Energy Dispersive Spectrometer', *Nucl. Instrum. Methods*, **165**, 63–65 (1979).
18. P. Lechner, C. Fiorini, R. Hartmann, J. Kemmer, N. Krause, P. Leutenegger, A. Longoni, H. Soltau, D. Stötter, R. Stötter, L. Strüder, U. Weber, Silicon drift detectors for high count rate X-ray spectroscopy at room temperature, *Nucl. Instrum. Methods A*, **458**, 281–287, (2001).
19. J. Nissenbaum, A. Holzer, M. Roth, M. Schieber, 'X-ray Fluorescence Analysis of High Z Materials with Mercuric Iodide Room Temperature Detectors', *Adv. X-ray Anal.*, **24**, 303–309 (1980).
20. P. Jalas, H. Sipila, S. Eranen, K. Leinonen, 'Near Room Temperature Energy-dispersive Detectors Processed on High-purity Silicon', *X-ray Spectrom.*, **24**(2), 63–69 (1995).
21. D.S. McGregor, H. Hermon, 'Room-temperature Compound Semiconductor Radiation Detectors', *Nucl. Instrum. Methods*, **295**, 101–124 (1997).
22. www.canberra.com, www.ketek.net, 2009.
23. B. Kanngießer, W. Malzer, I. Reiche, 'A New 3D Micro X-ray Fluorescence Analysis Set-up- First Archaeometric Applications', *Nucl. Instrum. Methods*, **B 211/2**, 259–264 (2003).
24. Ph. Potts, M. West (eds), *Portable X-ray Fluorescence Spectrometry*, RCS Publishing, 2008.
25. K. Tsuji, J. Injuk, R. Van Grieken, *X-ray Spectrometry Recent Technological Advances*, Wiley, 2004.
26. B. Holynska, 'Sampling and Sample Preparation in EDXRS', *X-ray Spectrom.*, **22**(4), 192–198 (1993).
27. J. Boman, P. Standzenieks, E. Selin, 'Beam Profile Studies in an X-ray Fluorescence Spectrometer', *X-ray Spectrom.*, **20**(6), 337–341 (1991).
28. R.D. Giaque, 'A Novel Method to Ascertain Sample Mass Thickness and Matrix Effects for X-ray Fluorescence Element Determinations', *X-ray Spectrom.*, **23**(4), 160–168 (1994).
29. R.D. Giaque, F. Asaro, F.H. Stross, T.R. Hester, 'High Precision Non-destructive X-ray Fluorescence Method Applicable to Establishing the Provenance of Obsidian Artifacts', *X-ray Spectrom.*, **22**(1), 44–53 (1993).
30. H.A. van Sprang, M.H.J. Bekkers, 'Determination of Light Elements Using X-ray Spectrometry. Part 1 – Analytical Implications of Using Scattered Tube Lines', *X-ray Spectrom.*, **27**(1), 31–36 (1997).
31. B. Vekemans, K. Janssens, L. Vincze, F. Adams, P. Van Espen, 'Analysis of X-ray Spectra by Iterative Least Squares (AXIL): New Developments', *X-ray Spectrom.*, **23**(6), 278–285 (1994).
32. G. Pepponi, C. Strelis, P. Wobrauschek, N. Zoeger, K. Luening, P. Pianetta, D. Giubertoni, M. Barozzi,

- M. Bersani, Nondestructive dose determination and depth profiling of arsenic ultrashallow junctions with total reflection X-ray fluorescence analysis compared to dynamic secondary ion mass spectrometry, *Spectrochim. Acta B*, **59**, 1243–1249 (2004).
33. R.W. Ryon, H.E. Martz, J.M. Hernandez, J.J. Haskins, E.J. Suoninen, 'Selection of the Method', in *Surface Characterization, A User's Sourcebook*, eds. D. Brune, R. Hellborg, H.J. Whitlow, O. Hunderi, Wiley-VCH, Weinheim, 14–31, 1997.